Synergistic, antagonistic and biocidal effects of amino (trimethylene phosphonic acid), polyacrylamide and Zn^{2+} on the inhibition of corrosion of mild steel in neutral aqueous environment

S. Rajendran, B.V. Apparao and N. Palaniswamy

The authors

S. Rajendran is with the Department of Chemistry, G.T.N. Arts College (Autonomous), Dindigul, Tamilnadu, India.

B.V. Apparao is with the Department of Chemistry, Regional Engineering College, Warangal, Andhrapradesh, India.

N. Palaniswamy is with the Corrosion Science and Engineering Division, Central Electrochemical Research Institute, Karaikudi, Tamilnadu, India.

Abstract

The corrosion rates of mild steel in a neutral aqueous environment containing 60 ppm $C1^-$ in the absence and presence of the sodium salt of amino (trimethylene phosphonic acid) (ATMP), polyacrylamide (PAA) and Zn^{2+} have been evaluated by the classical weight-loss method. The formulation consisting of 50 ppm PAA and 50 ppm Zn^{2+} and also the ATMP (300 ppm) –ZN^{2+} (50 ppm) system shows synergistic effect while the formulation consisting of 300 ppm ATMP and 50 ppm PAA shows antagonistic effect. The formulation consisting of 300 ppm ATMP, 50 ppm Zn^{2+} and 50 ppm PAA has 98 per cent corrosion inhibition efficiency and 99.9 per cent biocidal efficiency. The mechanistic aspects of corrosion inhibition are based, in a holistic way, on the results obtained from potentiostatic polarization study, X-ray diffraction technique, UV-visible, FTIR and luminescence spectra. Found that the protective film consists of FE^{2+}-ATMP complex, Fe^{2+}-PAA complex and $Zn(OH)_2$.

Anti-Corrosion Methods and Materials
Volume 44 · Number 5 · 1997 · pp. 308–313

Introduction

The adsorption behaviour of polyacrylamide (PAA) on gold and mild steel from sulphuric acid and hydrochloric acid has been studied using cyclic voltametry with simultaneous monitoring of the double layer capacity[1]. It has been reported that PAA strongly adsorbs on silver and titanium[2] and gold and iron[3] from aqueous neutral solutions. In acidic and neutral media, PAA has been used as corrosion inhibitor for iron[4]. The synergistic effect of PAA and hexamethylenetetramine has been reported[1]. Synergistic and antagonistic effects existing between 1-hydroxyethane-1, 1-diphosphonate, PAA and Zn^{2+} have been noticed[5]. In the present work the synergistic, antagonistic and biocidal effects existing between sodium salt of amino(trimethylene phosphonic acid) (ATMP), PAA and Zn2+ have been evaluated using the weight-loss method. The mechanistic aspects of inhibition of corrosion have been discussed, based on the results obtained from potentiostatic polarization study, X-ray diffraction technique, FTIR, UV-visible and luminescence spectra.

Experimental

Preparation of the specimens

Mild steel specimens (0.02 to 0.03 per cent S, 0.03 to 0.08 per cent P, 0.4 to 0.5 per cent Mn, 0.1 to 0.2 per cent C and the rest iron) of the dimensions $1 \times 4 \times 0.2$ cm were polished to a mirror finish and degreased with trichloroethylene and used for the weight-loss method and surface examination studies. For potentiostatic polarization studies, mild steel rod encapsulated in Teflon with an exposed cross section of 0.5 cm diameter was used as the working electrode. Its surface was polished to mirror finish and degreased with trichloroethylene.

Weight-loss method

Mild steel specimens, in triplicate, were immersed in 100 ml of the solutions containing various concentrations of the inhibitor in

One of the authors, S. Rajendran, thanks the University Grants Commission, New Delhi, India, for awarding a Fellowship, and to Ranjit Soundararajan, Correspondent, Professor S. Ramakrishnan, Principal and Professor P. Jayaram, H.O.D., Chemistry Department, G.T.N. Arts College (Autonomous), Dindigul for their encouragement.

Anti-Corrosion Methods and Materials
Volume 44 · Number 5 · 1997 · 308–313

the absence and presence of Zn^{2+}, for a period of seven days. The weights of the specimens before and after immersion were determined using Mettler balance, AE-240.

Potentiostatic polarization study
This study was carried out in a three electrode cell assembly connected to Bioanalytical system (BAS – 100A) electrochemical analyser, provided with IR compensation facility, using mild steel as the working electrode, platinum as the counter electrode and saturated calomel electrode as the reference electrode.

Surface examination study
The mild steel specimens were immersed in various test solutions for a period of two days. After two days, the specimens were taken out and dried. The nature of the film formed on the surface of the metal specimens was analysed by various surface analysis techniques.

The FTIR spectra
The FTIR spectra were recorded using Perkin-Elmer 1600 FTIR spectrophotometer.

The UV-visible spectra
The UV-visible reflectance spectra were recorded using Hitachi U-3400 spectrophotometer. The same instrument was used for recording UV-visible absorption spectra of aqueous solutions also.

X-ray diffraction technique
The XRD patterns of the film formed on the metal surface were recorded using a computer controlled X-ray powder diffractometer, JEOL JDX 8030 with CuK_{α} (Ni-filtered) radiation (λ = 1.5418 Å) at a rating of 40 kV, 20 mA. The scan rate was 0.05-20° per step and the measuring time was one second per step.

Luminescence spectra
The luminescence spectra of the film formed on the metal surface were recorded using Hitachi 650-10 S fluorescence spectrophotometer equipped with 150 W Xenon lamp and a Hamamatsu R 928 F photomultiplier tube. The emission spectra were corrected for the spectral response of the photomultiplier tube used and the excitation spectra recorded were corrected for the beam intensity variation.

Determination of the biocidal efficiency of the system
The biocidal efficiency of the system was determined using Zobell medium and calculating the number of colony forming units per ml, using a bacterial colony counter.

Results and discussion

Analysis of the results of the weight-loss method
Corrosion rates of mild steel in neutral aqueous environment containing 60 ppm Cl^- in the absence and presence of inhibitor and the inhibition efficiencies obtained by the weight-loss method and also the biocidal efficiencies of various environments are given in Table I. It is found that 50 ppm PAA has 53 per cent inhibition efficiency and 50 ppm Zn^{2+} is found to be corrosive. Interestingly, the formulation consisting of 50 ppm PAA and 50 ppm Zn^{2+} has 65 per cent inhibition efficiency. This indicates the synergistic effect existing between PAA and Zn^{2+}.

It is also observed that ATMP and Zn^{2+} show synergistic effect. However, quite interestingly, ATMP and PAA show antagonistic effect. This may be explained by the following facts:

(1) The complex formed between ATMP and PAA in solution has less tendency to break.
(2) The film (which is expected to consist of Fe^{2+}-ATMP complex and Fe^{2+}-PAA complex) formed on the anodic regions on the metal surface is constantly attacked by the aggressive chloride ions and broken.

It is interesting to note that the formulation consisting of 300 ppm ATMP, 50 ppm Zn^{2+} and 50 ppm PAA has 98 per cent inhibition efficiency and 99.9 per cent biocidal efficiency.

Analysis of potentiostatic polarization curves
The potentiostatic polarization curves of mild steel immersed in various environments are given in Figure 1. It is observed that the corrosion potential is shifted to the anodic side when PAA is added to the environment containing Cl^- or Cl^- and Zn^{2+}. However, the corrosion potential is shifted to the cathodic side (from –340 to –348 mV vs SCE) when PAA is added to the environment consisting of Cl^- and ATMP. The formulation consisting

Table I Corrosion rates of mild steel in neutral aqueous environment ($C1^-$ = 60 ppm) and in the absence and presence of inhibitor and the inhibition efficiencies obtained by the weight-loss method and the biocidal efficiencies of various environments

Sample number	ATMP ppm	Zn^{2+} ppm	PAA ppm	Corrosion rate mdd	Inhibition Efficiency (%)	Colony forming units/ml	Biocidal efficiency (%)
1.	0	0	0	15.54	–	10^8	–
2.	300	50	0	0.31	98	10^6	99
3.	300	50	50	0.29	98	10^5 to 10^6	99 to 99.9
4.	300	0	0	10.88	30	–	–
5.	0	50	0	19.11	–23	–	–
6.	0	0	50	7.30	53	–	–
7.	300	0	50	17.10	–10	–	–
8.	0	50	50	5.40	65	–	–

Figure 1 Potentiostatic polarization curves of mild steel immersed in various environments

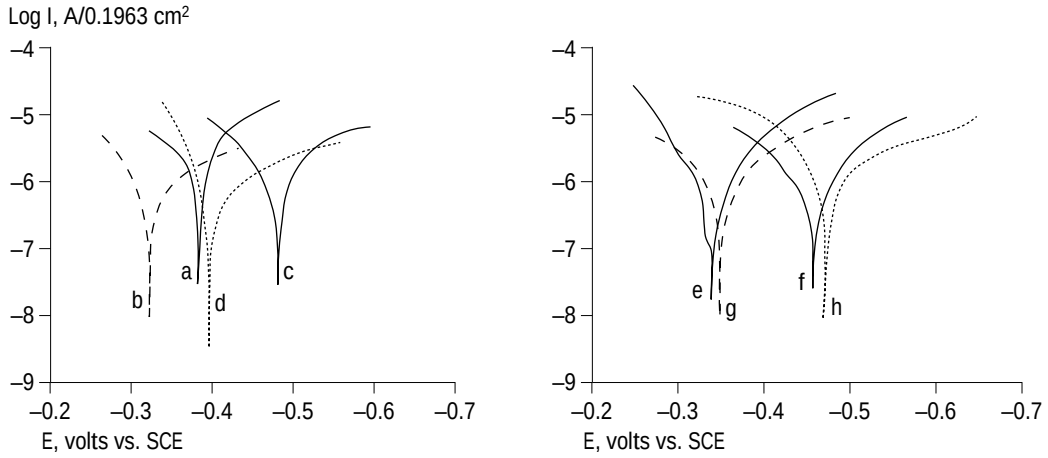

Key
(a) $C1^-$ 60 ppm
(b) $C1^-$ 60 ppm + PAA 50ppm
(c) $C1^-$ 60 ppm + Zn^{2+} 50ppm
(d) $C1^-$ 60 ppm + PAA 50ppm + Zn^{2+} 50ppm
(e) $C1^-$ 60 ppm + ATMP 300 ppm
(f) $C1^-$ 60 ppm + ATMP 300 ppm + Zn^{2+} 50ppm
(g) $C1^-$ 60 ppm + ATMP 300 ppm + PAA 50 ppm
(h) $C1^-$ 60 ppm + ATMP 300 ppm + PPA 50ppm + Zn^{2+} 50ppm

of 60 ppm Cl^-, 300 ppm ATMP, 50 ppm PAA and 50 ppm Zn^{2+} has the corrosion potential of –480 mV vs SCE. This potential is in between that of Cl^- alone (-389 mV vs SCE) and Cl^- -Zn^{2+} system (–489 mV vs SCE). This indicates that this formulation acts as mixed inhibitor. This is further supported by the fact that the anodic and cathodic Tafel slopes are shifted almost equally (≈25 mV/decade).

Analysis of UV-visible absorption spectra of solutions

The UV-visible absorption spectra of various systems are given in Figure 2. Change in position of the absorption maximum and or change in the value of absorbance indicate the formation a complex between two species in solution. Based on this principle, an analysis of Figure 2 reveals the formation of the following complexes in solution: Zn^{2+}– ATMP, Zn^{2+} – PAA, Fe^{2+} – ATMP, Fe^{2+} – PAA and ATMP-PAA.

Analysis of FTIR spectra

The FTIR spectra of pure ATMP and pure polyacrylamide (PAA) are given in Figures 3a and 3b. The FTIR spectrum of the film scratched from the surface of the metal specimen immersed in the environment consisting of 60 ppm Cl^-, 300 ppm ATMP and 50 ppm PAA is given in Figure 3c. It is found that the P-O stretching frequency of ATMP decreases from 1002 cm^{-1} to 974 cm^{-1} and the C-N

Figure 2 UV-visible absorption spectra of solutions

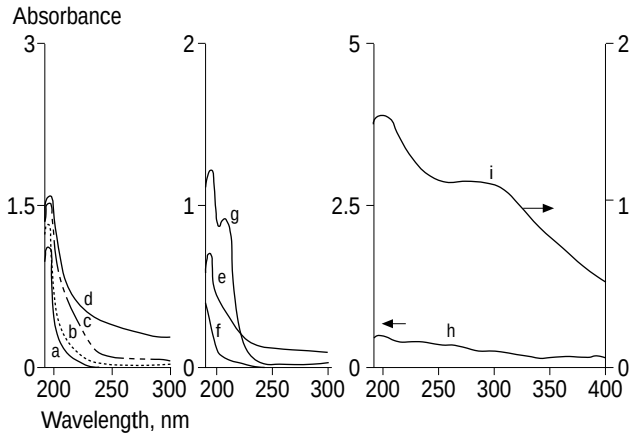

Key
(a) PAA 50 ppm
(b) PAA 50 ppm + Zn^{2+} 50 ppm
(c) PAA 50 ppm + ATMP 300 ppm
(d) PAA 50 ppm + Fe^{2+} 300 ppm
(e) ATMP 300 ppm
(f) Zn^{2+} 50 ppm
(g) ATMP 300 ppm + Zn^{2+} 50 ppm
(h) Fe^{2+} 300 ppm
(i) ATMP 300 ppm + Fe^{2+} 300 ppm

Figure 3 FTIR spectra of ATMP (a), PAA (b), and of mild steel surface immersed in various environments

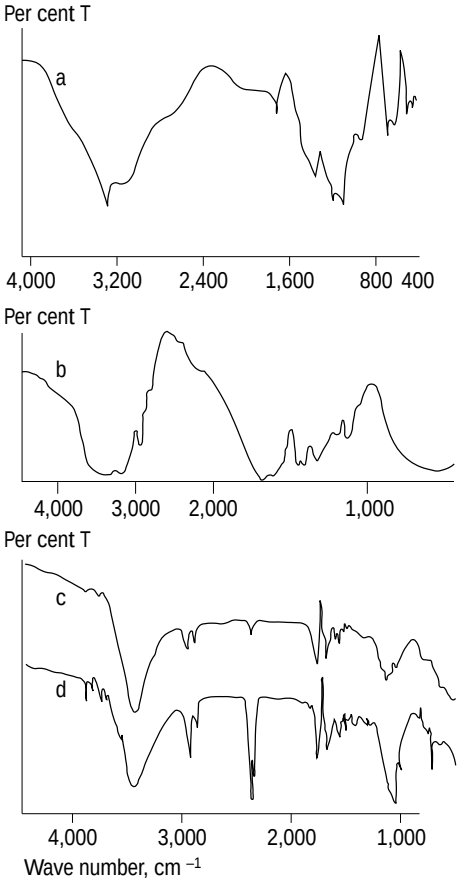

Key
(a) Pure ATMP
(b) Pure PAA
(c) $C1^{-}$ 60 ppm + ATMP 300 ppm + PAA 50 ppm
(d) $C1^{-}$ 60 ppm + ATMP 300 ppm + PAA 50 ppm + Zn^{2+} 50 ppm

stretching frequency of ATMP decreases from 1145 cm^{-1} to 1072 cm^{-1}[6-9]. These observations indicate that the O atom and N atom of ATMP are co-ordinated to Fe^{2+} resulting in the formation of Fe^{2+} – ATMP complex[9-13].

It is also observed that the C = O stretching frequency of PAA decreases from 1666.4 cm^{-1} to 1635.9 cm^{-1}, and the C-N stretching frequency of PAA increases from 1453.9 cm^{-1} to 1476.2 cm^{-1}. It is inferred that PAA is co-ordinated to Fe^{2+} through the O atom and not through N atom; the C-N bond acquires double bond character.

The FTIR spectrum of the film due to the environment consisting of 60 ppm Cl^{-}, 300 ppm ATMP, 50 ppm PAA and 50 ppm Zn^{2+} is given in Figure 3d. It is found that the P-O stretching frequency of ATMP decreases from 1002 cm^{-1} to 973.9 cm^{-1} and the C-N stretching frequency decreases from 1145 cm^{-1} to 1023.9 cm^{-1}. It is inferred that ATMP is co-ordinated to Fe^{2+} through the O and N atoms resulting in the formation of Fe^{2+} – ATMP complex[9-13].

The C = O stretching frequency of PAA decreases from 1666.4 cm^{-1} to 1652.3 cm^{-1} and the C-N stretching frequency increases from 1453.9 cm^{-1} to 1472 cm^{-1}. These observation suggest that PAA is co-ordinated to Fe^{2+} through the O atom and not through the N atom ; the C-N bond acquires double bond character. The peak at 1357 cm^{-1} is due to $Zn(OH)_2$[14].

Analysis of UV-visible reflectance spectra

The UV-visible reflectance spectra of the film formed on the surface of mild steel specimens immersed in various environments are given in Figure 4. The reflectance spectrum of the surface of the metal immersed in the environment containing 60 ppm Cl^{-}, 300 ppm ATMP and 50 ppm PAA is given in Figure 4a. The wavelength transition at 550 nm indicates that the brown film consists of oxides of iron[15-18] with a band gap of E_g = 1.239/0.55 = 2.25 eV having a semiconducting property[19-22]. The peak at 320 nm may be due to Fe^{2+}-PAA complex and the peak at 230 nm may be due to Fe^{2+}-ATMP complex.

The UV-visible reflectance spectra of the surface of the metal immersed in the environment consisting of 60 ppm Cl^{-}, 300 ppm ATMP, 50 ppm PAA and 50 ppm Zn^{2+} does not show wavelength transition at 550 nm, indicating absence of any oxides of iron on the metal surface. A thin interference film was

Figure 4 UV-visible reflectance spectra of mild steel surface immersed in various environments

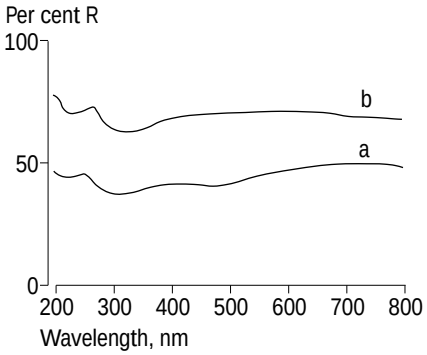

Key
(a) $C1^-$ 60 ppm + ATMP 300 ppm + PAA 50 ppm
(b) $C1^-$ 60 ppm + ATMP 300 ppm + PAA 50 ppm + Zn^{2+} 50 ppm

observed on the surface of the metal. The peaks at 320 nm and 230 nm may be due to Fe^{2+}-PAA complex and Fe^{2+}-ATMP complex respectively.

Analysis of the XRD patterns

The XRD patterns of the surface of the metal immersed in various environments are given in Figure 5. The XRD pattern of the surface of the metal immersed in the environment consisting of 60 ppm Cl^-, 300 ppm ATMP and 50 ppm PAA is given in Figure 5a. The peaks at $2\theta = 38.12^\circ$ and 60.67° correspond to γ- FeOOH. The peaks due to iron appear at $2\theta = 44.6^\circ$, 65.0° and 82.4°[23].

The XRD pattern of the surface of the metal immersed in the environment containing 60 ppm Cl^-, 300 ppm ATMP, 50 ppm PAA and 50 ppm Zn^{2+} shows the presence of iron peaks only ($2\theta = 44.6^\circ$, 65.0° and 82.3°)

Figure 5 XRD patterns of mild steel surface immersed in various environments

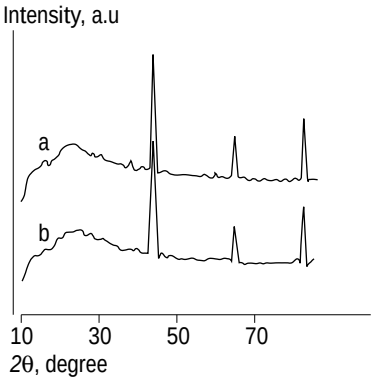

Key
(a) $C1^-$ 60 ppm + ATMP 300 ppm + PAA 50 ppm
(b) $C1^-$ 60 ppm + ATMP 300 ppm + PAA 50 ppm + Zn^{2+} 50 ppm

and the absence of oxides of iron such as α -FeOOH, γ-FeOOH and Fe_3O_4[23].

Analysis of the luminescence spectra

The luminescence spectra of the surface of the metal immersed in various environments are given in Figure 6. The emission spectrum (λ_{ex} = 300 nm) of the surface of the metal immersed in the medium consisting of 60 ppm Cl^-, 300 ppm ATMP and 50 ppm PAA is given in Figure 6a. This may be due to Fe^{2+}-ATMP and Fe^{2+}-PAA complexes embedded in γ- FeOOH. The corresponding excitation spectrum (λ_{em} = 400 nm) is given in Figure 6c.

The emission spectrum (λ_{ex} = 300 nm) of the surface of the metal immersed in the environment consisting of 60 ppm Cl^-, 300 ppm ATMP, 50 ppm PAA and 50 ppm Zn^{2+} is given in Figure 6b. This may be due to Fe^{2+}-ATMP and Fe^{2+}-PAA complexes in the presence of $Zn(OH)_2$. The corresponding excitation spectrum (λ_{em} = 460 nm) is given in Figure 6d.

Mechanism of inhibition of corrosion

Results of the weight-loss method reveal that the formulation consisting of 300 ppm ATMP, 50 ppm PAA and 50 ppm Zn^{2+} has 98 per cent corrosion inhibition efficiency. This formulation has 99 to 99.9 per cent biocidal efficiency. The polarization study shows that this formulation acts as a mixed inhibitor. The FTIR spectrum shows that the protective film

Figure 6 Luminescence spectra of mild steel surface immersed in various environments

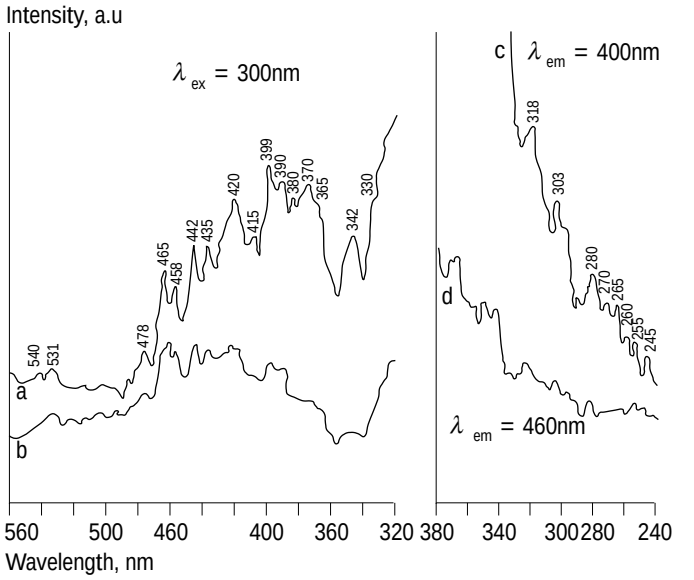

Key
(a) and (c) $C1^-$ 60 ppm + ATMP 300 ppm + PAA 50 ppm
(b) and (d) $C1^-$ 60 ppm + ATMP 300 ppm + PAA 50 ppm + Zn^{2+} 50 ppm

consists of Fe^{2+}-PAA and Fe^{2+}-ATMP complexes and $Zn(OH)_2$. The UV-visible reflectance spectrum and the XRD pattern indicate the absence of any oxides of iron. The protective film is found to be luminescent. In order to explain all these observations in a holistic way, the following mechanism of inhibition of corrosion has been proposed:

(1) When the environment consisting of 60 ppm Cl^-, 300 ppm ATMP, 50 ppm PAA and 50 ppm Zn^{2+} is prepared, there is formation of Zn^{2+}-ATMP complex and Zn^{2+}-PAA complex in solution.

(2) When the metal specimen is immersed in this environment, the above complexes diffuse from the bulk of the solution towards the metal surface.

(3) On the metal surface, Zn^{2+}-ATMP complex is converted into Fe^{2+}-ATMP complex on the local anodic region, as the latter is more stable than the former; Zn^{2+} is released.
Zn^{2+}-ATMP + $Fe^{2+} \rightarrow Fe^{2+}$-ATMP + Zn^{2+}

(4) Similarly, Zn^{2+}-PAA complex is converted into Fe^{2+}-PAA complex on the local anodic region, as the latter is more stable than the former.
Zn^{2+}-PAA + $Fe^{2+} \rightarrow Fe^{2+}$-PAA + Zn^{2+}
(formation of Fe^{3+}-ATMP and Fe^{3+}-PAA complexes to some extent cannot be ruled out.)

(5) The released Zn^{2+} is deposited as $Zn(OH)_2$ on the cathodic sites.
$Zn^{2+} + 2\ OH^- \rightarrow Zn(OH)2 \downarrow$

(6) Thus the protective film consists of Fe^{2+}-ATMP complex, Fe^{2+}-PAA complex and $Zn(OH)_2$.

Conclusions

The following points are concluded:

(1) Synergistic effect is noticed between ATMP and Zn^{2+} and also between PAA and Zn^{2+}.

(2) Antagonistic effect is noticed between ATMP and PAA.

(3) The formulation consisting of 300 ppm ATMP, 50 ppm PAA and 50 ppm Zn^{2+} has 98 per cent corrosion inhibition efficiency and 90 to 99.9 per cent biocidal efficiency.

(4) The protective film consists of Fe^{2+}-ATMP complex, Fe^{2+}-PAA complex and $Zn(OH)_2$ and is found to be luminescent.

References

1 Grchev, T., Cvetkovska, M., Stafilov, T. and Schultze, J.W., *Electrochim. Acta*, Vol. 36, 1991, p. 36.

2 Arsov, L., Grchev, T., Cvetkovska, M. and Petrov, G., *J. Serb. Chem. Soc.*, Vol. 48, 1983, p. 417.

3 Grchev, T., Cvetkovska, M. and Schultze, J.W., *Corros. Sci.*, Vol. 32, 1991, p. 103.

4 Sedahmed, G.H., Abd-El-Naby, B.A. and Abdel-Khalik, A., *Proc. 5th Europ. Symp. Corr. Inhibitors*, Vol. 1, Ferrara, Italy, 1980, p. 15.

5 Rajendran, S., Apparao, B.V. and Palaniswamy, N., *EUROCORR'96*, 24-26 September, Nice, France, 1996.

6 Silverstein, R.M., Bassler, G.C. and Morrill, T., *Spectrometric Identification of Organic Compounds*, John Wiley & Sons, New York, NY, 1981, p. 95.

7 Nakamoto, K., "Infrared and raman spectra of inorganic and coordination compounds", *Interscience*, John Wiley & Sons, New York, NY, 1986, p. 168.

8 Cross, A.D., "Introduction to practical infrared spectroscopy", *Scientific Publication*, Butterworths, London, 1960, p. 73.

9 Fang, J.L., Li, Y., Ye, X.R., Wang, Z.W. and Liu, Q., *Corros. Sci.*, Vol. 49, 1993, p. 266.

10 Rajendran, S., Apparao, B.V. and Palaniswamy, N., *Proc. 8th Europ. Symp. Corros. Inhibitors*, Vol. 1, Ferrara, Italy, 1995, p. 465.

11 Smith, T.D.J., *Inorg. Nucl. Chem.*, Vol. 9, 1959, p. 150.

12 Horner, L. and Horner, C.L., *Werkst. Korros.*, Vol. 27, 1976, p. 223.

13 Bohnsack, G., *UGB Kraftwerkstechnik*, Vol. 66, 1986, p. 48.

14 Sekine, I. and Kirakawa, Y., *Corrosion*, Vol. 42, 1986, p. 276.

15 Sharon, M., Tamizhmani, G. and Basaraswaram, K., *Proc. Indian Nat. Sci. Acd.*, Vol. 52, 1986, p. 311.

16 Sanchez, H.L., Steinfink, H. and White, H.S., *J. Solid State Chem.*, Vol. 41, 1982, p. 90.

17 Sharon, M. and Prasad, B.M., *Solar Energy Mat.*, Vol. 8, 1983, p. 457.

18 Sanchez, C., Sieber, K.D. and Somorjai, G.A., *J. Electroanal. Chem.*, Vol. 252, 1988, p. 269.

19 Schultze, W. and Stimming, U., *Z. Phys. Chem.*, Vol. 98, 1975, p. 285.

20 Wilhelm, S.M., Yun, K.S., Ballenger, L.W. and Hackerman, N., *J. Electrochem. Soc.*, Vol. 126, 1979, p. 416.

21 Wilhelm, S.M. and Hackerman N., *J. Electrochem. Soc.*, Vol. 128, 1981, p. 1668.

22 Abrantes, L.M. and Peter, L.M., *J. Electroanal. Chem.*, Vol. 150, 1983, p. 593.

23 Favre, M. and Landolt, D., *Corros. Sci.*, Vol. 34, 1993, p. 1481.